JOURNAL OF MATERIALS SCIENCE 29 (1994) 5745–5756

Synthesis and pyrolysis of polysilazane as the precursor of Si_3N_4/SiC ceramic

Y. C. SONG, Y. ZHAO, C. X. FENG, Y. LU
The Department of Materials Science and Applied Chemistry, Changsha Institute of Technology, Changsha, Hunan, People's Republic of China

By co-ammonolysis of $MeHSiCl_2$ and Me_2SiCl_2 and following thermal polymerization, polysilazanes as the precursors to Si_3N_4/SiC ceramic fibre were synthesized. The tendency to cross-link in thermal polymerization is suppressed as the result of the introduction of Me_2SiCl_2 as a starting material. The reactions occurring during thermal polymerization of ammonolysis products are discussed based on infrared (i.r.) and ^1H nuclear magnetic resonance (NMR) spectra analysis. The pyrolysis process of polysilazanes is examined in nitrogen and in an NH_3 atmosphere. It is shown that the formation of SiC results from the pyrolysis of $Si–CH_3$ groups in polysilazanes by means of the formation of $Si–CH_2–Si$ intermediate bonds. The structure and properties of ceramics derived from the pyrolysis of polysilazane and polycarbosilane in N_2 or NH_3 atmosphere are compared and discussed. Si–N–C ceramic, which was proved to be a composite of α-Si_3N_4 and β-SiC, exhibits better thermal stability at temperatures higher than 1300 °C.

1. Introduction

In recent years, preparation of ceramics by the pyrolysis of an organic polymer has attracted considerable attention and has become a steadily growing field. After SiC and SiC–TiC fibres were successfully synthesized from polycarbosilane and polytitanocarbosilane, commercially referred to by the tradenames Nicalon and Tyranno [1, 2], respectively, much attention has focused on the preparation of silicon nitride (Si_3N_4) fibres by the pyrolytic transformation of polysilazane (PSZ) precursors. Nicalon fibre, as well known, is not a pure SiC fibre; the presence of excess carbon and oxygen affect its mechanical properties and causes degradation of its tensile strength at elevated temperatures [3, 4]. Therefore, recent progress in preparing Si_3N_4 fibres concentrate on the synthesis of suitable polysilazane and on the preparation of high purity Si_3N_4 fibres. For instance, research workers of the American Dow Corning Corp. and the Japanese Toa Nenryo Kogyo Corp. developed a process whereby two kinds of ceramic fibres with compositions approaching Si_3N_4 were synthesized from precursors hydridopolysilazane and perhydropolysilazane, respectively [5, 6]. These fibres have high tensile strength and elastic modulus comparable to the Nicalon fibre, and may be expected to have higher thermal and oxidation stabilities.

Silicon nitride is well known for its excellent chemical inertness, thermal shock resistance and hardness. These characteristic properties make it suitable for many applications similar to SiC. On the other hand, one of the advantages of the method of preparing ceramics from an organic polymer, is the ability to vary ceramic composition by varying polymer composition. Therefore, it is more convenient to prepare a composite of Si_3N_4 and SiC, that is the Si_3N_4/SiC composite ceramic, by this method. This material may be expected to exhibit some new properties that are different from Si_3N_4 or SiC alone.

In fact, as early as 1973, an $Si_xN_yC_z$ fibre was obtained by Verbeek from a polycarbosilazane precursor [7]. Afterwards, Seyferth and Wiseman reported the synthesis of polysilazane with $Si–CH_3$ functional groups from the ammonolysis product of methyldichlorosilane, $MeSiHCl_2$, in the presence of catalysts. Pyrolysis of this polysilazane gives a ceramic material which is a mixture of Si_3N_4, SiC and C in yields of 80–85% [8]. Many experiments have also shown that the presence of $Si–CH_3$ groups in polysilazanes results in the production of SiC along with Si_3N_4 when pyrolysed under an inert atmosphere [9, 10]. Obviously, Si_3N_4/SiC composite ceramics can be prepared from polysilazane with $Si–CH_3$ groups, and the composition of these ceramics should be changed by varying the content of $Si–CH_3$ groups in the polysilazane.

In an attempt at preparing this polysilazane, it was found that the ammonolysis product of $MeHSiCl_2$ could be converted easily into polysilazane by heating in the absence of any catalysts. However, this thermal polymerization proceeded so rapidly that an unmelted rubbery solid was obtained. Only when dimethyldichlorosilane, Me_2SiCl_2, was introduced as a starting material, did the polymerization become controllable and suitable polysilazanes were obtained. In this paper, the synthesis of polysilazanes by thermal polymerization of the co-ammonolysis products of $MeHSiCl_2$ and Me_2SiCl_2, which are the relatively

0022–2461

cheap, commercially available organochlorosilanes, are reported. The structure and properties of the polysilazanes obtained, and the characteristics of the reaction in the thermal polymerization, are examined. The pyrolysis process of the polysilazanes under N_2 or NH_3 atmosphere are also studied. In addition, thermal stability of ceramics derived from polysilazane and polycarbosilane (PC) as the precursor of the SiC fibre at elevated temperature are compared and discussed.

2. Experimental procedure

2.1. Polymer synthesis

First, $MeHSiCl_2$ and Me_2SiCl_2 were mixed in different molar ratios with benzene in a three-necked flask with a reflux condenser and a thermometer. After the air in the flask had been replaced with dry N_2 gas, NH_3 gas was introduced into this system accompanied by highspeed stirring. The temperature of the system rose to about 80 °C over a 1 h period, some reflux was observed at 80 °C. After ammonia was added for about 2 h, the system slowly cooled to room temperature. The reaction mixture was filtered to remove ammonium chloride (NH_4Cl). Benzene was distilled off and the ammonolysis product as viscous liquid, was obtained. Then, the ammonolysis product was put into a reaction vessel with a quartz reactor tube and heated slowly in a nitrogen gas flow. The low boiling species in the ammonolysis product was further reacted in the heated quartz tube to increase their molecular weight; and then they were refluxed into the reaction vessel or selected as liquid oligomer after cooling. After thermal polymerization were carried out at a specific temperature between 300 to 480 °C for 1–1.5 h, the PSZ products, as transparent pale yellow or brown solids were obtained.

2.2. Pyrolysis of the polysilazanes

The PSZ sample was placed in a quartz boat in a tube furnace equipped with a temperature controller. Pyrolysis was conducted in a nitrogen gas flow of $1\,l\,min^{-1}$. The sample was heated at a rate of $150\,°C\,h^{-1}$ to a specific temperature between 300 to 1300 °C and held at this temperature for 1 h; or, the sample was thermally cross-linked under a nitrogen atmosphere at 500 °C. The resultant cross-linked product was ground into fine powder. Then, these powders were heat treated in an NH_3 gas flow of $1\,l\,min^{-1}$ to a specific temperature between 300 to 1000 °C, with a 1 h hold at this temperature. To examine the thermal stability of ceramics derived from polymer precursors at elevated temperature, three kinds of ceramics, that is the pyrolysis products of PSZ under N_2 gas up to 1300 °C and under NH_3 gas atmosphere up to 1000 °C accompanied by further treatment under N_2 gas up to 1300 °C, as well as the pyrolytic product of polycarbosilane under N_2 gas up to 1300 °C, were further heat treated up to 1500 °C in an argon gas flow and kept at this temperature for 1 h.

2.3. Measurements

The infrared (i.r.) spectra of samples were measured using an Hitachi 270–30 infrared spectrophotometer with a fixed thickness (0.2 mm) cell of KBr in CCl_4 solution or by the KBr disc method.

Number average molecular weights ($\bar{M}_n$) of samples were measured with a corona 114 molecular weight apparatus by vapour phase osmometry (VPO) in a toluene solution. The molecular weight distributions were measured using a Watters-244 liquid chromatograph with Ultrastyragel as the gel–permeation chromatograph (GPC) column in toluene solution.

^1H and ^{29}Si nuclear magnetic resonance (NMR) spectra of the samples were obtained on an R-24B high resolution NMR spectrometer at 60 MHz with deuterated chloroform as a solvent and tetramethylsilane (TMS) as an external reference.

Thermogravimetric–differential thermal analysis (TGA–DTA) curves of samples were obtained by a Rigaku TGA–DTA thermal analyser in $40\,cm^3\,min^{-1}$ nitrogen flow up to 900 °C, at a heating rate of $10\,°C\,min^{-1}$. Thermogravimetric analysis cure of a sample treated under NH_3 atmosphere was found by measuring weight loss during pyrolysis.

Carbon, hydrogen and nitrogen analyses were performed on a PE 2400 CHN elemental analyser.

X-ray diffraction (XRD) patterns of the pyrolysis products were measured with a Siemens D-500 automatic X-ray diffractometer using CuK_α radiation.

3. Results and discussion

3.1. Ammonolysis reaction and structure of products

The ammonolysis of organochlorosilanes is a well known reaction. In the ammonolysis of Me_2SiCl_2 and $MeHSiCl_2$, or co-ammonolysis of Me_2SiCl_2 and $MeHSiCl_2$ in different molar ratios as shown in Table I, it was observed that when NH_3 gas was introduced into the benzene solution of reactants, the reaction occurred immediately accompanied by the formation of an NH_4Cl white precipitate and by the evolution of heat. The temperature of the system rose to about 80°C, the boiling point of benzene, and then reduced slowly to room temperature; which shows the completion of the ammonolysis. After NH_4Cl and solvent were removed by filtration and distillation, respectively, the ammonolysis products (AP) were obtained. I.r. spectra of the products are shown in Fig. 1: absorptions are at 2960, 2900 and $1410\,cm^{-1}$ (C–H); 1260, 825, 690 and $630\,cm^{-1}$ (Si–CH_3 and Si–C); 3400 and $1180\,cm^{-1}$ (N–H); and $920\,cm^{-1}$ (Si–N–Si). In the i.r. spectra of AP-2 and AP-5, the absorption of $2150\,cm^{-1}$ (Si–H) is also observed. The appearance of absorption peaks due to N–H and Si–N–Si bonds indicates the formation of an Si–NH–Si structure in the ammonolysis products.

The ammonolysis of diorganodichlorosilanes, R_2SiCl_2(R = alkyl and aryl), cyclic products $(R_2SiNH)_n$ are usually formed in preference to polymers. In the case of Me_2SiCl_2, products have been proved to be a mixture of hexamethylcyclotrisilazane $(Me_2SiNH)_3$ and octamethylcyclotetrasilazane

TABLE I Ammonolysis conditions and characterization of products

Ammonolysis product	$Me_2SiCl_2/MeHSiCl_2$ (molar ratio)	Si-H/Si-CH_3 (molar ratio in reactants)	Si-H/Si-CH_3[a] (molar ratio)	MeSiMe(H)/NH[a] (molar ratio)
AP-1	1:0	0.00	0.00	0.98[b], 1.00[c]
AP-2	1:1	0.33	0.36	1.65
AP-3	1:2	–	–	–
AP-4	1:3	0.60	0.57	2.96
AP-5	0:1	1.00	1.02	2.85

[a] Calculated value based on the ^1H NMR spectra of ammonlysis products.
[b] Liquid.
[c] Solid.

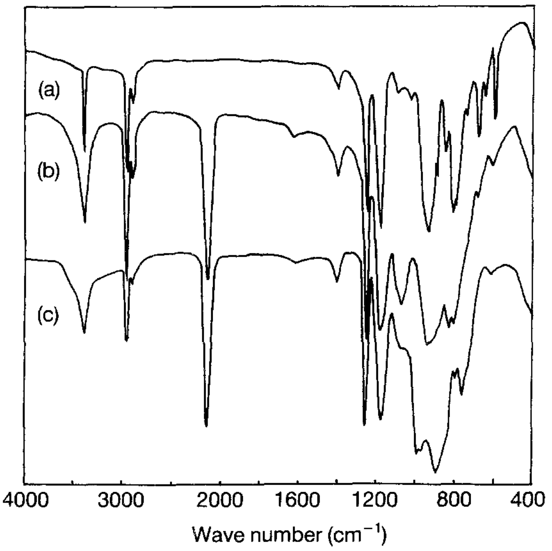

Figure 1 Infrared spectra of ammonolysis products (a) AP-1, (b) AP-2, (c) AP-5.

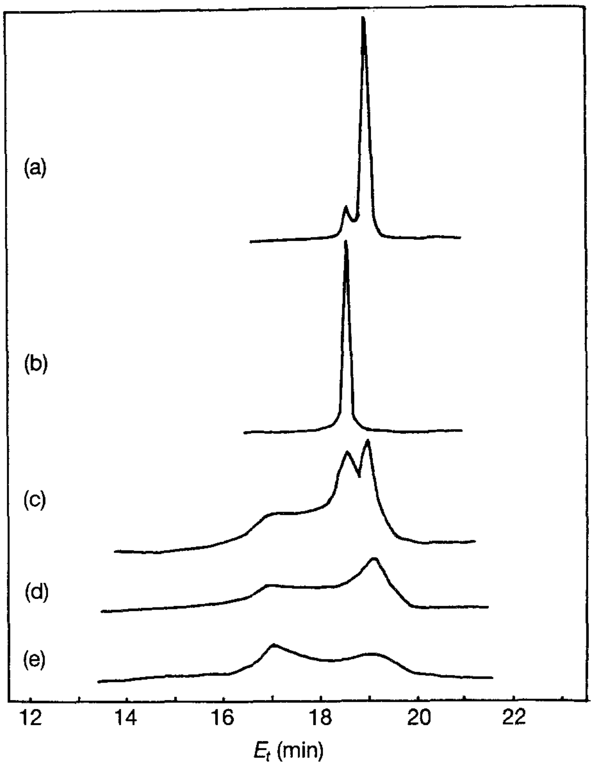

Figure 2 Molecular weight distribution of ammonolysis products: (a) AP-1 (liquid); (b) AP-1 (solid); (c) AP-2; (d) AP-4; (e) AP-5.

$(Me_2SiNH)_4$ [11]. In these experiments, it was found that the ammonolysis of Me_2SiCl_2 yielded a transparent liquid product and a white crystal solid. Sharp peaks in the GPC patterns (see Fig. 2a, b) show that both products have a single molecular structure. Their molecular weights were found by VPO to be 212 and 284, respectively; evidently, the liquid product is $(Me_2SiNH)_3$ (M = 219) and the solid one $(Me_2SiNH)_4$ (M = 292).

However, as shown in Fig. 2e, the ammonolysis product of $MeHSiCl_2$, AP-5, seems not to have such a single molecular structure in these experimental conditions. The broad peak in the GPC pattern shows the formation of oligomer with a complicated structure. While the co-ammonolysis products of Me_2SiCl_2 and $MeHSiCl_2$, e.g. AP-2 and AP-4, are intermediate between AP-1 and AP-5, in which the cyclic structure $(M_2SiNH)_3$, $(Me_2SiNH)_4$ and more complicated structure are contained.

To have a better understanding of the structure of the ammonolysis products, ^1H NMR spectra were measured. Fig. 3b shows Si–CH_3 protons (0.05–0.3 p.p.m.) and N–H protons (0.4 p.p.m.) resonance in ammonolysis product of Me_2SiCl_2. In ^1H NMR spectra of $MeHSiCl_2$ ammonolysis products, or its mixture with Me_2SiCl_2, e.g. Fig. 3a, multiplets between 4.3 and 5.0 p.p.m. due to Si–H proton resonance can also be observed. Based on the integrated intensity ratios in these ^1H NMR spectra, the molar ratios of Si–H/Si–CH_3, as well as MeSiMe(H)/N–H, can be obtained, as shown in Table I.

The structure of the $MeHSiCl_2$ ammonolysis product has been identified as $(MeSiHNH)_n$, where $n = 3, 4$ and 5 [11]. If the co-ammonolysis products of Me_2SiCl_2 and $MeHSiCl_2$ had similar structures, that is $[MeSiMe(H)/NH]_n$, the molar ratio of MeSiMe(H)/N–H in products would be 1; but these ratios are always greater than 1 as seen from Table I, except for the ammonolysis product of Me_2SiCl_2 which have cyclic structure $(SiMe_2/NH)_n$ as stated above.

It has been reported that in the ammonolysis of H_3SiCl or H_2SiCl_2, the initially formed disilazane is unstable and disproportionates to give ammonia and a product with trisubstituted nitrogen [12]. In these experiments, ammonolysis products underwent distillation up to about 120 °C to remove solvent; so, it is

TABLE II Synthesis conditions, molecular weight and spinnability of polysilazane

PSZ	$Me_2SiCl_2/MeHSiCl_2$ (molar ratio)	Reaction temperature[a] (°C)	$\bar{M}_n$	Spinnability[b]
PSZ-1	1:0	480	1275	Good
PSZ-2	1:1	410	1625	Good
PSZ-3	1:2	370	1960	Poor
AP-4	1:3	340	Cross-linking	Unspinnable
AP-5	0:1	300	Cross-linking	Unspinnable

[a] Reaction time, 1 h

[b] Good, could be spun evenly; poor, spinnable, but breakage of filament occurred frequently.

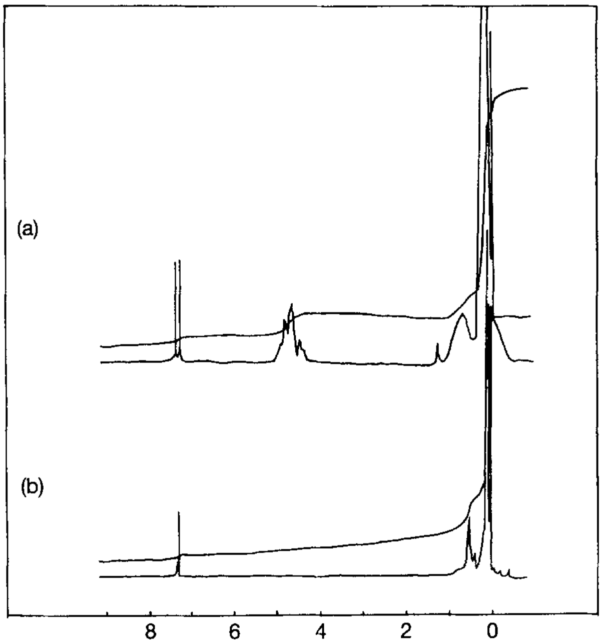

Figure 3 ^1H NMR spectra of ammonolysis products: (a) AP-2; (b) AP-1.

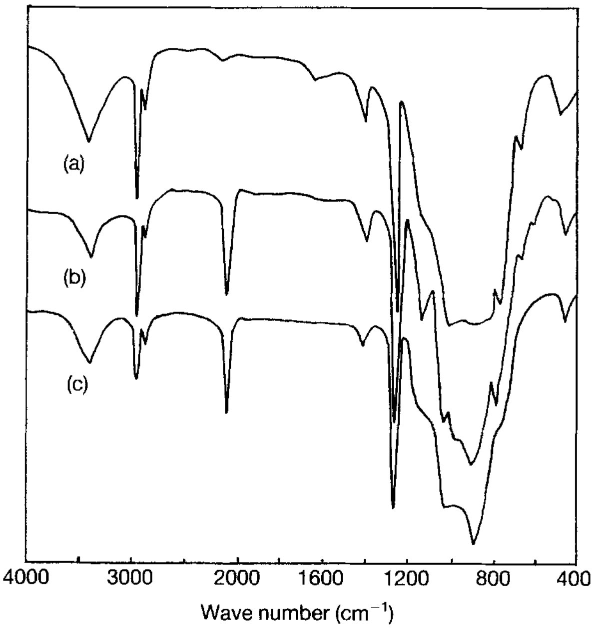

Figure 4 Infrared spectra of polysilazanes: (a) PSZ-1; (b) PSZ-2; (c) PSZ-5.

reasonable to consider that, in the ammonolysis or co-ammonolysis, the initially formed structure MeSiHNH may undergo similar disproportionation due to being heated to give a more complicated structure with a $(MeSiH)_{1.5}N$ structural unit. In fact, as seen from Table I, the molar ratios of $SiH/Si{-}CH_3$ are almost constant in products compared with reactants, it means that the Si–H and $Si{-}CH_3$ bonds are not involved in further changes of product structure; therefore, the increase in molar ratio of MeSiMe(H)/N–H are attributed to the decrease of N–H bonds, as a result of disproportionation in structure which results in the evolution of NH_3 gas.

From the above discussion, the ammonolysis products of $MeHSiCl_2$ and its mixture with Me_2SiCl_2 can be considered as a complex mixture, containing cyclic compounds such as $(Me_2SiNH)_n$, $(MeHSiNH)_n$ ($n = 3$, 4 and 5) as well as oligomer with $(MeSiH)_{1.5}N$ structural unit.

3.2. Synthesis of polysilazanes

To be used as a precursor to ceramic materials, the ammonolysis products must be converted to polysilazanes which have higher molecular weight and desired processability, e.g. solubility, meltability and spinnability, which is necessary to prepare ceramic fibres. Such polysilazanes can be obtained by the thermal polymerization of co-ammonolysis products of $MeHSiCl_2$ and Me_2SiCl_2. The synthesis conditions and properties of the PSZs are shown in Table II. It is seen that with increasing Me_2SiCl_2 content in the starting materials, the tendency to cross link polymers is restrained, PSZs with good spinnability are obtained. On the other hand, reactivity of the ammonolysis product decreases, so that higher reaction temperatures are required. Suitable PSZs can be produced from co-ammonolysis products when the reactants $Me_2SiCl_2/MeHSiCl_2$ molar ratio is in the range of 1:1 to 1:2.

I.r. spectra of PSZs derived are shown in Fig. 4. Compared with i.r. spectra of AP (Fig. 1), a remarkable decrease in absorption peaks at 3400, 1180 cm^{-1} (N–H), and 2150 cm^{-1} (Si–H), and the appearance of an absorption peak of 1040 cm^{-1}, which is attributed to the Si_3N structure, can be seen. The same change can be observed either in PSZ-1, or in PSZ-2, or in PSZ-5.

To examine thermal polymerization in more detail, the reaction process during conversion of AP-2 to

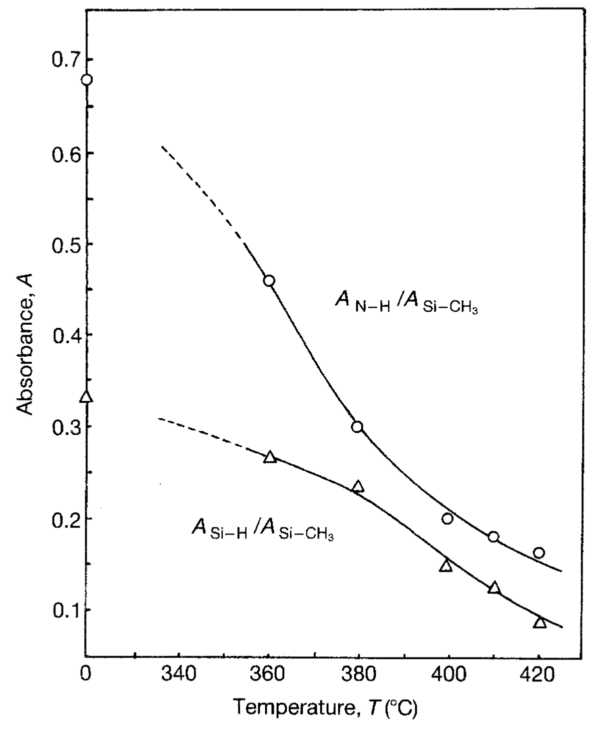

Figure 5 Change in absorbance A_{N-H}/A_{Si-CH_3} and A_{Si-H}/A_{Si-CH_3} with reaction temperature during conversion of AP-2 to PSZ-2 by thermal polymerization.

PSZ-2 was followed by measuring the reactant i.r. spectra and GPC patterns at different temperatures. The results are shown in Figs 5 and 6. In Fig. 5, the absorbance of Si–CH_3 (1260 cm^{-1}) is selected as an inner standard for which little change in polymerization is shown; the Si–H (2150 cm^{-1}) and N–H (1180 cm^{-1}) absorbancies decrease as the reaction temperature increases; at the same time, the content of high molecular weight components in PSZ increase and the lower molecular weight species decrease (Fig. 6). This suggests that the polymerization of ammonolysis products results from reaction of Si–H and N–H bonds. Seyferth and Wiseman reported that adjacent N–H and Si–H groups in the ammonolysis product of $MeHSiCl_2$ will undergo a so-called dehydrocyclodimerization (DHCD) reaction in the presence of basic catalysts such as KH, which may be represented by the following equation [8]

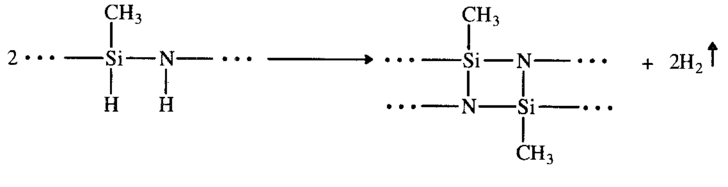
(1)

$$2\cdots\underset{\text{H}}{\overset{\text{CH}_3}{\text{Si}}}-\underset{\text{H}}{\text{N}}\cdots \longrightarrow \begin{array}{c}\cdots\overset{\text{CH}_3}{\text{Si}}-\text{N}\cdots\\ \cdots\text{N}-\underset{\text{CH}_3}{\text{Si}}\cdots\end{array} + 2\text{H}_2\uparrow \qquad (1)$$

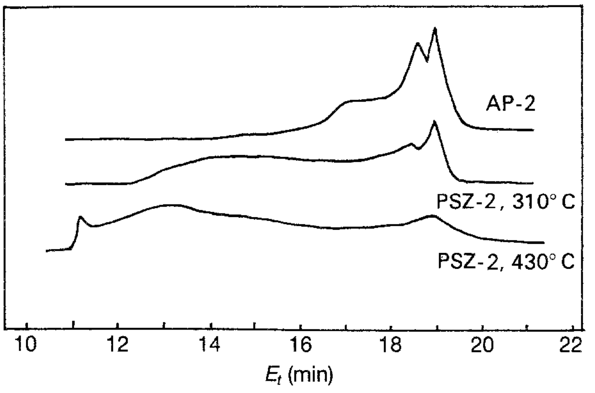

Figure 6 GPC patterns of AP-2 and PSZ obtained at different temperature from AP-2.

This reaction leads to an increase of molecular weight and to the liberation of hydrogen. The changes in absorbance A_{Si-H} and A_{N-H} shown in Fig. 5 and the evolution of hydrogen detected by gas chromatography (GC) indicate that the Equation 1 also occurs during thermal polymerization. As already described in Section 3.1., there exist three kinds of structural units Me_2SiNH, MeSiHNH and $(MeSiH)_{1.5}N$, in co-ammonolysis products of $Me_2Si_2Cl_2$ and $MeHSiCl_2$. So, Equation 1 takes place between MeSiHNH units. From Fig. 6, it is observed that two peaks at 18.6 and 19.0 min of elution time in the GPC pattern of AP-2, which are attributed to the cyclic structures, $(Me_2SiNH)_4$ and $(Me_2SiNH)_3$ separately, are weakened and eventually disappear with increasing reaction temperature; correspondingly, a broad peak appears at high molecular weights. Obviously, a reaction in which the structural unit Me_2SiNH is involved occurs. As Me_2SiNH is surrounded with MeSiHNH or $(MeSiH)_{1.5}N$ units, this reaction may be considered to be a dehydrocoupling reaction between structural unit Me_2SiNH and MeSiHNH or $(MeSiH)_{1.5}N$, that is between inadjacent NH and Si–H groups

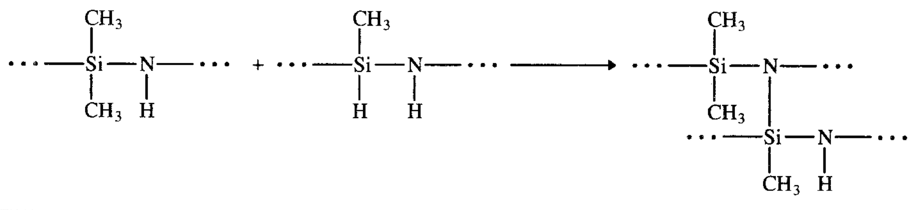
(2)

$$\cdots\underset{\text{CH}_3}{\overset{\text{CH}_3}{\text{Si}}}-\underset{\text{H}}{\text{N}}\cdots + \cdots\underset{\text{H}}{\overset{\text{CH}_3}{\text{Si}}}-\underset{\text{H}}{\text{N}}\cdots \longrightarrow \begin{array}{c}\cdots\underset{\text{CH}_3}{\overset{\text{CH}_3}{\text{Si}}}-\text{N}\cdots\\ \cdots\underset{\text{CH}_3}{\text{Si}}-\underset{\text{H}}{\text{N}}\cdots\end{array} + \text{H}_2\uparrow \qquad (2)$$

From Equations 1 and 2, it can be seen that the N–H and Si–H groups in ammonolysis products provide the functionality which permits the molecular weight to be increased. Therefore, cross-linking PSZs which have very high molecular weight were produced from AP-4 and AP-5, which have a higher content of Si–H and N–H bonds. In the case of AP-2 and AP-3, the

Si–H bonds content is decreased as the result of the introduction of the Me_2SiNH unit. Thus, tendency to cross-link is suppressed and PSZs of suitable molecular weight can be obtained.

When the Si–H groups are absent, e.g. in the case of AP-1, which is a mixed cyclic structure of $(SiMe_2NH)_3$ and $(SiMe_2NH)_4$, thermal polymerization become so difficult that higher reaction temperatures or longer reaction times are required. A change in the infrared spectrum of AP-1 during thermal polymerization is shown in Fig. 7. The reaction temperature is kept at 360 °C, the absorption peak at $1180\,cm^{-1}$ decreases with increasing reaction time; at the same time, absorption in the vicinity of $1040\,cm^{-1}$ due to the Si_3N structure increases. It is apparent that the consumption of N–H bonds results in the formation of Si_3N structure. Changes in N–H ($1180\,cm^{-1}$) and $Si–CH_3$ ($1260\,cm^{-1}$) absorbance are shown in Fig. 8, together with $\bar{M}_n$. Corresponding with decreasing N–H absorbance, an increase in $\bar{M}_n$ is seen, while no change in $Si–CH_3$ absorbance can be observed. This indicates that $Si–CH_3$ bonds do not participate in thermal polymerization; the increasing molecular weight of the reaction system can only be attributed to reaction of N–H bonds, which results in combination between molecules by means of Si_3N structure. This reaction may be expressed in the following

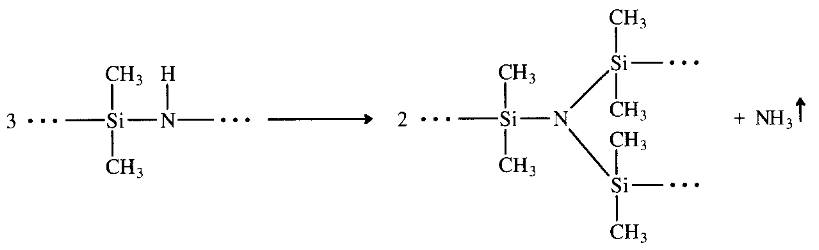

(3)

In thermal polymerization, AP-1 undergoes such disproportionation as to increase its molecular weight and to convert it into polysilazane PSZ-1.

As already discussed in Section 3.1., in co-ammonolysis Me_2SiCl_2 and $MeHSiCl_2$ products, a part of the MeSiHNH unit has undergone such disproportionation that it turns into the $(MeSiH)_{1.5}N$ structure. Consequently, relating to the discussion above, it is reasonable to consider that, apart from Equations 1 and 2, MeSiHNH and Me_2SiNH units containing co-ammonolysis products will continue in Equation 3.

The ^1H NMR spectra of polysilazanes were measured, the molar ratios of $Si–H/Si–CH_3$, $N–H/Si–CH_3$ and N–H/Si–H in PSZ-2 and PSZ-5 are found based on these NMR spectra and are shown in Table III. By comparison with corresponding ratios in AP-2 and AP-5, the decrease of Si–H and N–H bonds after thermal polymerization can be seen, which is consistent with i.r. spectral analysis. Furthermore, the AP molar ratios of N–H/Si–H decrease after conversion to PSZs, instead of remaining constant, suggesting that disproportionation reactions take place in thermal polymerization. This reaction leads to a more rapid consumption of N–H bonds than Si–H bonds, which can also be observed from Fig. 5. In the case of AP-5, the same change shows that the structural unit MeSiHNH has undergone such disproportionation in thermal polymerization.

From the above discussion, it may be seen that thermal polymerization of ammonolysis products is a complicated reaction. Not only will the DHCD reaction occur between adjacent Si–H and N–H bonds, but a dehydrocoupling reaction takes place between adjacent Si–H and N–H bonds. Furthermore, a disproportionation reaction, resulting in condensation of molecules, is also present in $SiMe_2NH$ or MeSiHNH structural units.

The ^{29}Si NMR spectrum of PSZ was measured. Si–O resonance, in addition to Si–N and Si–C resonance, was observed; it showed the presence of a small amount of oxygen in PSZ. Table IV shows the elemental composition of PSZs. It is evident that the composition of PSZs is affected by synthesis conditions, especially by the $Me_2SiCl_2/MeHSiCl_2$ molar ratio in the starting materials. When this ratio decreases, the content of Si and N will increase and that of C and H decrease.

Due to the complexity of thermal polymerization stated above, it is difficult to give the composition of polysilazane structural units. In fact, due to the reactions shown in Equations 1–3, new structural units, such as MeSiN, $(Me_2Si)_{1.5}N$, $(Me_2Si)(MeSiH)_{0.5}N$, $(MeHSi)(Me_2Si)_{0.5}N$, etc., are produced and remain in PSZs. However, it is reasonable to infer the general structure of PSZ as follows, based on the above examination

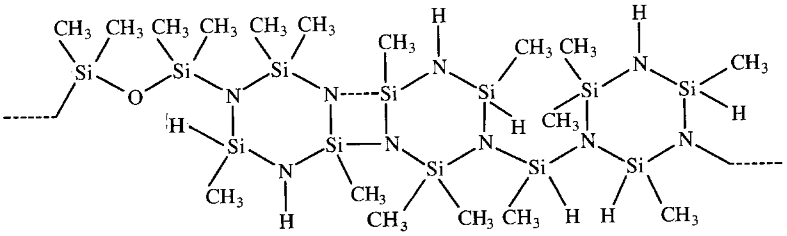

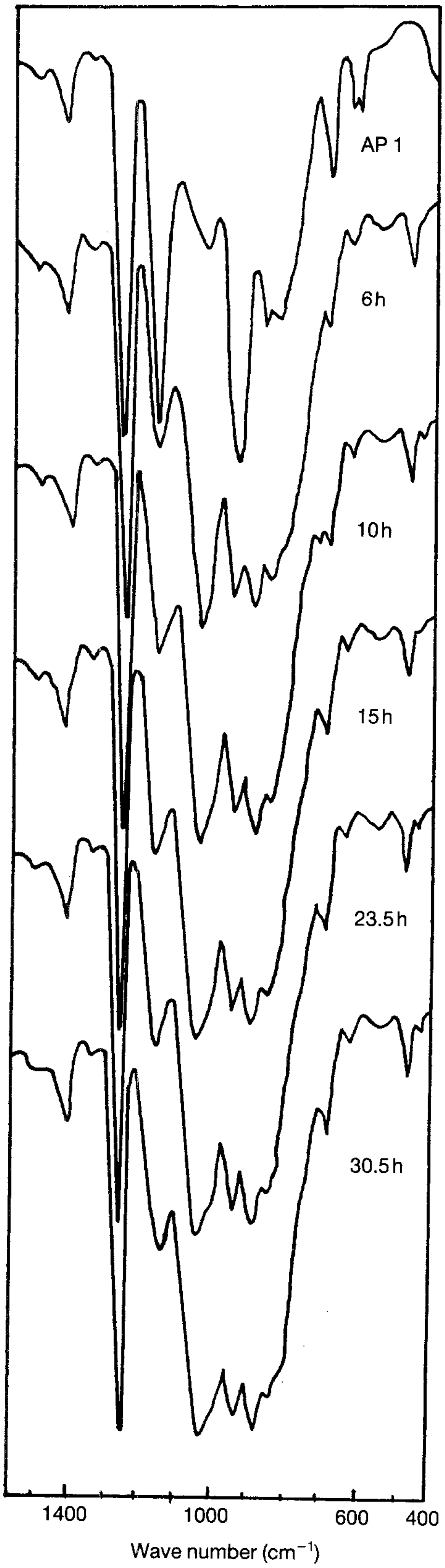

Figure 7 Change in the infrared spectra of AP-1 during thermal polymerization at 360 °C.

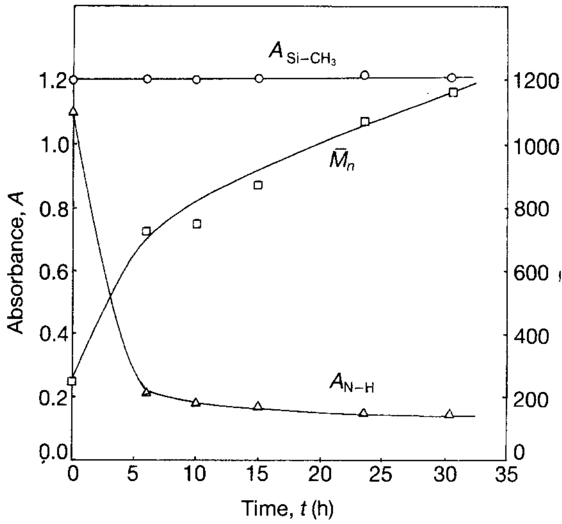

Figure 8 Change in absorbance A_{N-H}, A_{Si-CH_3} and M_n with reaction time, t, during conversion of AP-1 to PSZ by thermal polymerization at 360 °C.

TABLE III Characterization of polysilazane

Sample	SiH/Si-CH$_3$ (molar ratio)	N-H/Si-CH$_3$ (molar ratio)	N-H/Si-H (molar ratio)
AP-2	0.360	0.414	1.150
PSZ-2	0.188	0.158	0.840
AP-5	1.020	0.358	0.351
PSZ-5[a]	0.965	0.261	0.270

[a] Synthesized from AP-5 at 220 °C for 5 h, $\bar{M}_n = 700$.

TABLE IV The elemental composition (wt %) and empirical formulae of polysilazanes

Sample[a]	Si	N	C	H	Empirical formula
PSZ-1	31.89	13.96	32.78	7.51	$Si_{1.0}N_{0.88}C_{2.4}H_{6.6}$
PSZ-2	38.13	17.24	27.33	7.71	$Si_{1.0}N_{0.90}C_{1.7}H_{5.7}$
PSZ-5	47.65	18.40	19.29	5.55	$Si_{1.0}N_{0.77}C_{0.94}H_{3.3}$

[a] A part of oxygen is present in PSZs.

3.3. Pyrolysis of polysilazane

The pyrolytic behaviour of polysilazane is dependent on its structure and composition. TGA curves of PSZ-1, PSZ-2 and PSZ-5 are shown in Fig. 9. A remarkable difference in the TGA curves reveals the effect of the side groups present in PSZs on the pyrolysis process and ceramic yields. Cross-linked PSZ-5 is stable and has no weight loss up to about 550 °C; so, a higher ceramic yield (84% at 900 °C) is obtained. Whereas for PSZ-1, because the Si–H group is absent, which provides the reactivity to permit the molecules to be cross-linked, a great weight loss below 400 °C is shown due to the escape of volatile low molecular weight oligomer and a lower ceramic yield, e.g. 65% at 900 °C. In the case of PSZ-2, though it has not cross-linked as in PSZ-5, a higher ceramic yield as the result of the presence of Si–H and N–H side groups with latent chemical reactivity, is shown.

To examine the pyrolysis of polysilazanes, the pyrolysis process of PSZ-2 was followed by measuring i.r. spectra of its pyrolysis products at different temperatures in a nitrogen atmosphere. The results are shown in Fig. 10. The changes of side groups, Si–CH$_3$ and Si–H groups in PSZ may be observed by plotting the absorbance at 2150 cm^{-1}, A_{Si-H}, and at 1260 cm^{-1}, A_{Si-CH_3}, against the heat treatment temperature, as shown in Fig. 11. The TGA–DTA curve of PSZ-2 was also measured as shown in Fig. 12. Relating Fig. 12 to Figs 10 and 11, it is seen that the

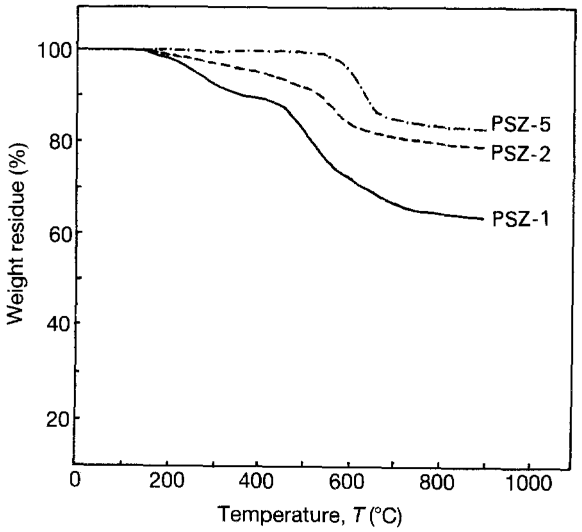

Figure 9 TGA curves of polysilazane in nitrogen atmosphere.

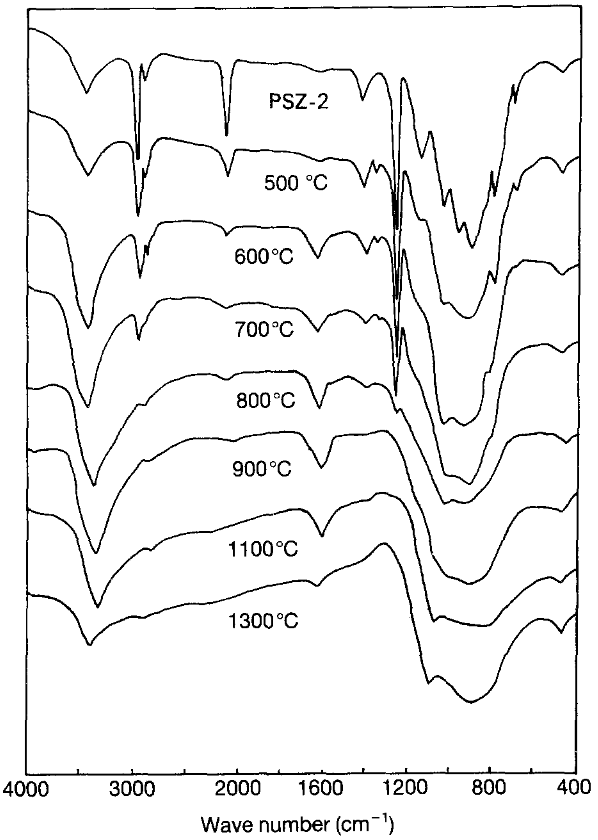

Figure 10 Infrared spectra of pyrolysis products of PSZ-2 at different temperatures in nitrogen atmosphere.

pyrolysis of polysilazane can be divided roughly into three stages. In the first stage (200–500 °C), the DTA curve shows disorderly peaks and weight loss begins in the TGA curve, corresponding to decreasing absorption peaks of the Si–H, N–H and Si–CH_3 bonds in the i.r. spectra. The experiment shows that the molecular weight of PSZ increases with increasing temperature, and that it turns into an insoluble and unmelted solid at 500 °C, accompanied by the escape of a certain amount of low molecular weight pieces. It is apparent that condensation polymerization taking place in the synthesis of PSZ continues to occur at this stage, resulting in the cross-linking of PSZ molecules.

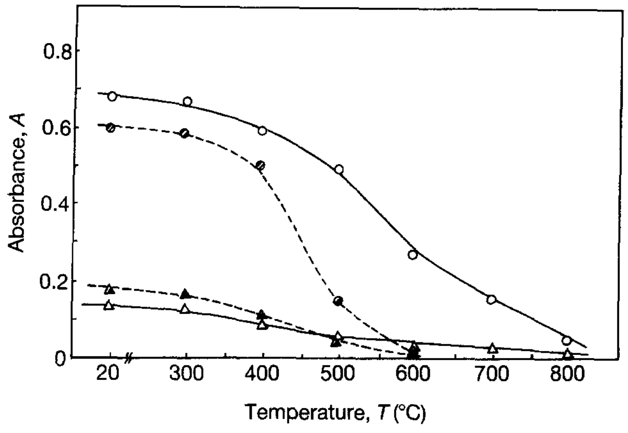

Figure 11 Change in absorbance $A_{\mathrm{Si-CH_3}}$ and $A_{\mathrm{Si-H}}$ with temperature during pyrolysis of polysilazane in nitrogen and ammonia gas atmosphere, respectively: (○) $A_{\mathrm{Si-CH_3}}$, N_2; (●) $A_{\mathrm{Si-CH_3}}$, NH_3; (△) $A_{\mathrm{Si-H}}$, N_2 and (▲) $A_{\mathrm{Si-H}}$, NH_3.

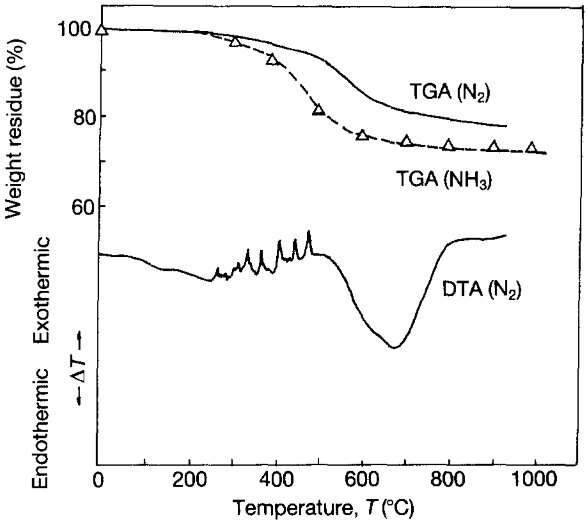

Figure 12 TGA-DTA curve of PSZ-2 in nitrogen atmosphere and TGA curve of PSZ-2 in ammonia atmosphere.

The weight loss is mainly caused by evaporation of low molecular weight polysilazane. In the second stage (500–800 °C), a large endothermic peak centred at about 700 °C appears in the DTA curve. Correspondingly, a larger weight loss can be observed in the TGA curve. In the i.r. spectra (Figs 10 and 11), the absorbances of Si–H, Si–CH_3 and N–H decrease rapidly until their disappearance at 800 °C; while absorption at about 1040 cm^{-1} due to Si_3N bonds increases relatively. The evolution of H_2 and CH_4 were also detected by GC analysis. These results demonstrate that this state is a main pyrolysis stage of PSZ. In this stage, breakage and decomposition of the side groups in PSZ, such as Si–CH_3, Si–H and N–H bonds, occur accompanied by dehydrogenation and demethanation; a network structure with Si–N–Si skeleton bonds forms, and PSZ are converted into an inorganic structure. In the third stage (900–1300 °C), no large change is observed in the i.r. spectra; only the absorption peak of the Si–O bonds (1080 and 460 cm^{-1}) and the overlapping peak of the Si–N bonds (950 cm^{-1}) and Si–C bonds (825 cm^{-1}) are present in the i.r. spectrum of the pyrolysis product at

1300 °C as shown in Fig. 10. Elemental analysis shows that the C, H and N contents (wt %) in this pyrolysis product are 17.80, 0.21 and 23.70, respectively. As will be described later, the pyrolysis product is an amorphous Si–N–C ceramic which can be converted into a composite of α-Si_3N_4 and β-SiC crystalline at higher temperatures.

The results above-mentioned reveal that pyrolysis of polysilazane with Si–N–Si skeleton bonds and Si–CH_3 side groups under N_2 atmosphere, results in the production of a Si_3N_4/SiC composite ceramic instead of a pure Si_3N_4 ceramic. Evidently, the carbon in Si–CH_3 side groups in polysilazane is not released completely as methane during pyrolysis; it will be partly turned into carbon present in the Si–C–Si skeleton in a particular way. In fact, in the i.r. spectrum of PSZ-2 heat treated at 500 °C in N_2 atmosphere (Fig. 10), a new absorption peak at 1360 cm^{-1} appears, which can be attributed to Si–CH_2–Si bonds; this peak is also observed in the i.r. spectra of other PSZs synthesized at different Me_2SiCl_2/$MeHSiCl_2$ molar ratios when they are further treated at 500 °C, even though sometimes it is so small that it is easily ignored. As it is absent from the original PSZs, the Si–CH_2–Si bond should be produced by reaction of Si-H and Si–CH_3 or Si–CH_3 alone, which is assumed to be

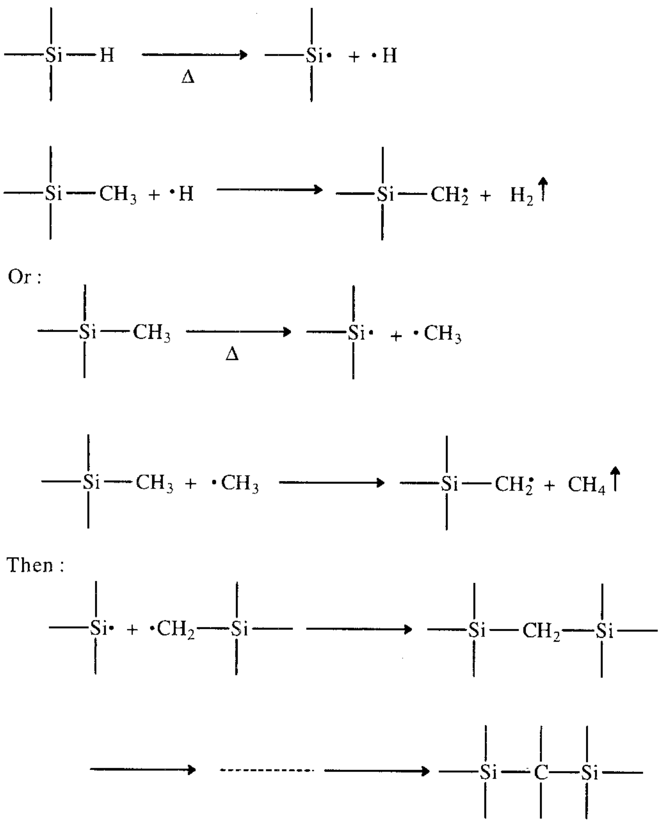

$$\equiv Si{-}H \xrightarrow[\Delta]{} \equiv Si\cdot + \cdot H$$

$$\equiv Si{-}CH_3 + \cdot H \longrightarrow \equiv Si{-}CH_2^{\cdot} + H_2\uparrow$$

Or:

$$\equiv Si{-}CH_3 \xrightarrow[\Delta]{} \equiv Si\cdot + \cdot CH_3$$

$$\equiv Si{-}CH_3 + \cdot CH_3 \longrightarrow \equiv Si{-}CH_2^{\cdot} + CH_4\uparrow$$

Then:

$$\equiv Si\cdot + \cdot CH_2{-}Si\equiv \longrightarrow \equiv Si{-}CH_2{-}Si\equiv$$

$$\longrightarrow \cdots\cdots \longrightarrow \equiv Si{-}\overset{|}{\underset{|}{C}}{-}Si\equiv$$

The decrease in the C and H content of PSZ-1 and PSZ-2 after heat treatment at 500 °C, which is seen from comparison of Table V with Table IV, is consistent with the above assumption. This is also a reaction taking place in pyrolysis of polycarbosilane [13], a precursor of the SiC fibre. Thus, apart from the Si–N–Si network structure, a three-dimensional structure with an Si–C–Si skeleton is also formed by Si–CH_2–Si intermediate links and, eventually, a composite of Si_3N_4–SiC ceramic is obtained.

TABLE V The elemental composition of PSZs and their pyrolysis products

Sample	PSZ[a] (wt %)			Pyrolysis products[b] (wt %)		
	C	H	N	C	H	N
PSZ-1	28.62	6.83	15.77	19.67	0.30	19.48
PSZ-2	25.96	7.15	18.20	17.80	0.21	23.70
PSZ-3	24.15	6.64	20.39	14.39	0.34	25.03

[a] PSZs were cross-linked at 500 °C for 1 h.
[b] Pyrolysis conditions: N_2, 1300 °C, 1 h.

As the formation of SiC comes from the pyrolysis of Si–CH_3 groups, it is possible to decrease the content of SiC in the ceramic derived by decreasing the Si–CH_3 content in PSZs. The elemental composition of PSZs and their pyrolysis products up to 1300 °C (see Table V) show that the lower the carbon content in the precursor PSZs, the lower the carbon content and the higher the nitrogen content become in the pyrolysis products. The organic carbon present in PSZs, in the form of Si–CH_3 groups, is transformed into inorganic carbon existing in SiC, at an almost constant ratio of 60–70%.

The carbon content of pyrolysis products can be further reduced by pyrolysis of PSZ in NH_3 atmosphere. It was reported previously that polycarbosilane can be turned into an Si–N–O ceramic by pyrolysis in an NH_3 atmosphere [14]. The pyrolysis of the hydridopolysilazane in NH_3 atmosphere yields an amorphous, low carbon silicon nitride powder [15]. In these experiments, the pyrolysis process of PSZs in NH_3 gas is also followed by i.r. spectroscopy. The changes of Si–CH_3 and Si–H groups in PSZ-2 during pyrolysis under NH_3 atmosphere are also shown in Fig. 11, compared with pyrolysis under N_2 atmosphere, it can be seen that the pyrolysis of Si–CH_3 and Si–H bonds has been moved up. At 400 °C, the absorbance of Si–H and Si–CH_3 begins to decrease remarkably; at 600 °C, these bonds tend to disappear, correspondingly, a large weight loss is observed in the temperature range 400–600 °C in the TGA curve (Fig. 12). Evidently, conversion to an inorganic structure is completed at a lower temperature in an NH_3 atmosphere than in an N_2 atmosphere. Another characteristic property shown during pyrolysis under an NH_3 atmosphere is decarbonization. Elemental analysis showed that the carbon content in the pyrolysis product is lower than 1 wt % when it is heat treated above 600 °C.

3.4. Thermal stability of the Si–N–C ceramic

As above, a silicon-based ceramic was obtained by pyrolysis of PSZ in an N_2 atmosphere at 1300 °C, which consists of silicon, nitrogen, carbon and a small amount of hydrogen and oxygen; whereas a low carbon silicon-based ceramic was produced by pyrolysis in NH_3 gas flow up to 1000 °C accompanied by further heat treatment under an N_2 atmosphere up to

1300 °C. For comparison, another silicon-based ceramic was made by pyrolysis of polycarbosilane in an N_2 atmosphere at 1300 °C. These three kinds of ceramics are designated as Si–N–C, Si–N and Si–C ceramics, respectively, based on their composition. Of course, a small amount of oxygen and hydrogen are present in these ceramics.

The i.r. spectra of these ceramics are shown in Fig. 13; the Si–C ceramic exhibits absorptions at 1080 cm^{-1} (Si–O stretching) and at 825 cm^{-1} (Si–C stretching). Compared with it, the Si–N ceramic (Fig. 13c) shows an overlapping absorption peak of Si–O bonds (1080 cm^{-1}) and Si–N bonds (950 cm^{-1}); while, in i.r. spectra of the Si–N–C ceramic (Fig. 13b), absorption of Si–C bonds are also observed along with Si–O and Si–N bonds. Comparison of i.r. spectra reveals the difference in composition of these three kinds of ceramics.

The X-ray diffraction (XRD) patterns of these ceramics are shown in Fig. 14, the three diffraction peaks at $2\theta = 35.5$, 60 and 72° appear in Si–C ceramic, which are due to (1 1 1), (2 2 0) and (3 1 1) diffraction of β-SiC, respectively; but no clear diffraction peak can be observed in XRD patterns of Si–N and Si–N–C ceramics. This indicates that these two ceramics should be amorphous in structure. As compared with Si–C ceramics produced at the same temperature, it seems that crystallization of the ceramic is restrained by the introduction of nitrogen.

In order to investigate the thermal stability of ceramics at elevated temperature, these three kinds of ceramic produced from organosilicon polymer were heat treated in an argon atmosphere at and above 1300 °C. The i.r. spectra of the three kinds of ceramic heat treated at 1500 °C shown in Fig. 15, are indicative of decreasing Si–O absorption and of a relative increase in Si–C and Si–N absorption. Both the Si–C and Si–N–C ceramics show no obvious weight loss during heat treatment up to 1500 °C; whereas the Si–N ceramic exhibits a detectable weight loss (about 9%). XRD patterns of these ceramics treated at 1500 °C in an argon atmosphere are shown in Fig. 16; the diffraction peaks of the Si–C ceramic become sharper as a result of increasing heat treatment temperature, the corresponding apparent crystallite size of β-SiC, L_{111}, which is found out by the well known Scherrer equation, is 7.08 nm; this is larger than that of Si–C ceramic before heat treatment, which is 4.06 nm. Evidently, crystal growth has occurred in the Si–C ceramic. Concerning the Si–N ceramic, the same crystal growth is also observed by comparing Fig. 14c with Fig. 16c. The XRD pattern shown in Fig. 16c is completely identical to that of pure α-Si_3N_4; it indicates that the Si–N ceramic has transformed rapidly

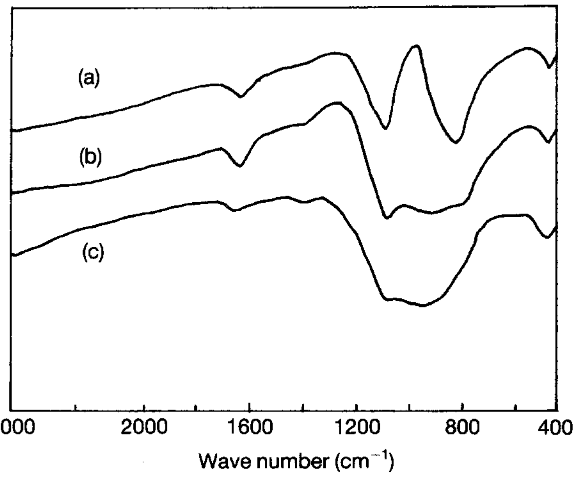

Figure 13 I.r. spectra of (a) Si–C ceramic, (b) Si–N–C ceramic and (c) Si–N ceramic.

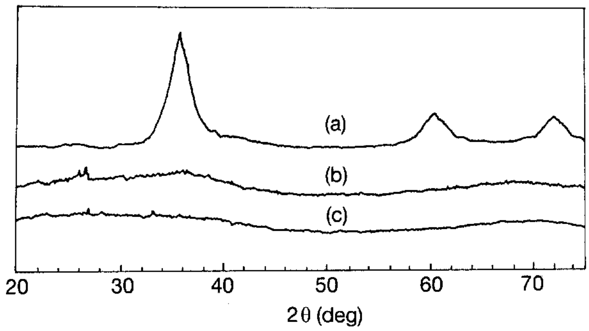

Figure 14 X-ray diffraction patterns (CuK_α) of (a) Si–C ceramic, (b) Si–N–C ceramic and (c) Si–N ceramic.

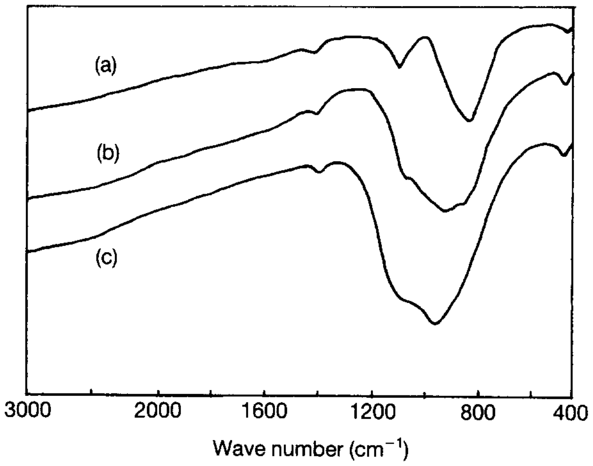

Figure 15 I.r. spectra of (a) Si–C ceramic, (b) Si–N–C ceramic and (c) Si–N ceramic heat-treated at 1500 °C.

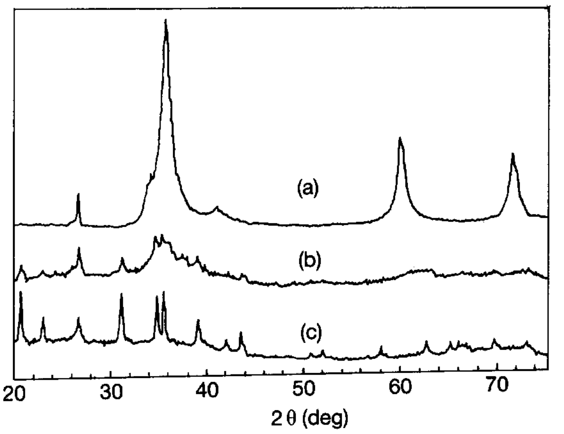

Figure 16 X-ray diffraction patterns (CuK_α) of (a) Si–C ceramic, (b) Si–N–C ceramic and (c) Si–N ceramic heat-treated at 1500 °C in argon atmosphere.

TABLE VI Elemental composition (wt %) of ceramics

Sample	Before heat treatment			Treated at 1400 °C			Treated at 1500 °C		
	C	H	N	C	H	N	C	H	N
Si–N–C ceramic	14.74	0.41	23.48	14.61	0.21	23.80	14.45	0.00	24.04
Si–N ceramic	0.62	0.30	28.25	0.77	0.15	32.40	0.35	0.13	35.38

into an α-Si_3N_4 crystal from its original amorphous state. At the same time, the composition of the Si–N ceramic shows a relevant change, as shown in Table VI; the nitrogen content of the Si–N ceramic treated at 1500 °C is close to that of pure Si_3N_4. As regards the Si–N–C ceramic, as shown in Fig. 16b, the appearance of diffraction peaks at $2\theta = 31$, 34.5 and 35.5° due to α-Si_3N_4 show the presence of α-Si_3N_4; the broad diffraction peaks at $2\theta = 35.5$, 60 and 72° indicate the formation of a β-SiC microcrystal (L_{111} is about 2.0 nm). It is apparent that the Si–N–C ceramic heat treated at 1500 °C is a composite of α-Si_3N_4 and β-SiC, whose composition can be calculated to be 36.4% SiC, 60.1% Si_3N_4 and 3.5% C (by weight) based on the assumption that no free silicon is present in this ceramic.

It has been reported that ceramic materials obtained using preceramic polymer processing, e.g. the Nicalon SiC fibre, which was manufactured by pyrolysis of a polycarbosilane precursor, will produce a remarkable decrease in tensile strength when subjected to heat treatment beyond 1300 °C in an inert atmosphere [3, 4]; this phenomenon is considered as a result of structural instability, which can be attributed to the fact that this material is not of high purity and excess carbon and oxygen exist in addition to SiC. At elevated temperatures, the following reaction between oxygen and excess carbon will take place [16]

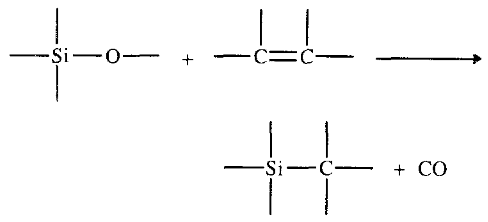

$$-\mathrm{Si}-\mathrm{O}- + -\mathrm{C}=\mathrm{C}- \longrightarrow -\mathrm{Si}-\mathrm{C}- + \mathrm{CO}$$

This reaction results in the evolution of CO gas and promotes crystallization and the crystal growth of β-SiC, which lead to the formation of defects, thereby lowering fibre strength. The above-mentioned changes in the Si–C ceramic above 1300 °C is the case.

It was reported that silicon oxynitride fibre obtained from a polycarbosilane fibre would decompose to silicon nitride and a SiO and N_2 gas phase at elevated temperatures [14]. In the case of the Si–N ceramic, as a result of the presence of oxygen, which is confirmed by the appearance of Si–O bonds absorption peaks in Fig. 13 and by the diffraction peak at $2\theta = 26.6°$ in Fig. 16c due to a (1 0 1) diffraction of the α-quartz, similar decomposition occurs as well, resulting in rapid transformation towards pure α-Si_3N_4 accompanied by an observable weight loss and rapid crystal growth.

From the above discussion, it may be seen that both Si–C and Si–N ceramics are unstable systems at elevated temperatures due to the occurrence of harmful reactions and rapid crystal growth, and this is attributed to the presence of oxygen as a detrimental impurity.

However, in the case of the Si–N–C ceramic, although a small amount of oxygen is present in the ceramic, which can be confirmed by i.r. spectra and by the X-ray diffraction pattern as well, harmful reactions, as mentioned above, are negligible because no obvious weight loss is detected, and the carbon and nitrogen contents are almost constant after heat treatment as shown in Table VI. Especially, though the grains have grown sufficiently in the Si–C and Si–N ceramics, this effect is remarkably restrained in the Si–N–C ceramic heat treated at the same temperature, so that a microcrystalline state of β-SiC and α-Si_3N_4 is obtained. Consequently, it may be considered that, as harmful reactions and grain growth are suppressed effectively in the Si–N–C ceramic system, this composite Si_3N_4 and SiC structure has better thermal stability.

From the above-mentioned observations and discussion, it seems that polysilazanes synthesized from co-ammonolysis products of Me_2SiCl_2 and $MeHSiCl_2$ are suitable precursors of Si_3N_4/SiC ceramic materials, e.g. fibre, coating and binder. In practice, the Si_3N_4/SiC fibre has been obtained from precursor PSZ-2 and PSZ-3. The diameter, tensile strength and Young's modulus of these fibres were 8–10 μm, 1.0–1.3 GPa, 100–120 GPa, respectively. Further structural characterization and advancement of this fibre is in progress.

4. Conclusions

Synthesis and the pyrolytic characteristic of polysilazanes prepared by thermal polymerization of co-ammonolysis products of $MeHSiCl_2$ and Me_2SiCl_2 have been studied. When Me_2SiCl_2, which is a relatively cheap starting material, is introduced, the tendency to cross-link in thermal polymerization is suppressed and polysilazanes having desired processability is obtained. Thermal polymerization is a complicated reaction, not only will a dehydrocoupling reaction occur between adjacent or unadjacent Si–H and N–H bonds, but a disproportionation reaction is present in structural units containing N–H bonds. Polysilazane prepared in such a way contains Si–CH_3, Si–H and N–H side groups in its Si–N–Si backbond, whose pyrolysis in an N_2 atmosphere at 1300 °C leads to an amorphous Si–N–C ceramic and in an NH_3 atmosphere, to a low carbon silicon-based ceramic. Si–CH_3

side groups in polysilazane are converted into Si–C–Si inorganic skeleton during pyrolysis through the formation of Si–CH_2–Si intermediate bonds. Therefore, the SiC content of the derived ceramic can be changed by adjusting the Si–CH_3 content is polysilazane. At temperatures higher than 1300 °C, the Si–C ceramic obtained from polycarbosilane, and the Si–N ceramic from pyrolysis of polysilazane in an NH_3 atmosphere form unstable structural system due to the occurrence of harmful reactions and rapid crystal growth; however, the Si–N–C ceramic, which is a composite of α-Si_3N_4 and β-SiC, exhibits better thermal stability.

References

1. T. TERANISHI, H. ICHIKAWA and T. ISHIKAWA, *New Mater. New Processes* **2** (1983) 379.
2. T. YAMAMURA, *Polym. Prepr.* **25** (1984) 6.
3. S. M. JOHNSON, R. D. BRITTAIN, R. H. LAMOREAUX and D. J. ROWCLIFFE, *J. Amer. Ceram. Soc.* **71** (1988) C-132.
4. T. MAH, H. L. HECHT, D. E. MCCULLUM and J. R. HOENIGMAN, *J. Mater. Sci.* **19** (1984) 1191.
5. G. E. LEGROW, T. F. LIM, J. LIPOWITZ and R. REAOCH *Amer. Ceram. Soc. Bull.* **66** (1987) 363.
6. T. ISODA, H. KAYA, M. ARAI, H. NISHII and O. FUNAYAMA, in "Proceedings of the First Japanese International SAMPE Symposium, Chiba, 28 November–1 December 1989", edited by N. Igata, I. Kimpara, T. Kishi, E. Nakata, A. Okura and T. Urgu (Society for the Advancement of Materials and Process Engineering, Tokyo, Japan) p. 912.
7. W. VERBEEK, US Pat. 3853567 (Dec. (1974).
8. D. SEYFERTH and G. H. WISEMAN, *J. Amer. Ceram. Soc.* **67** (1984) C-132.
9. G. WINTER, W. BERBEEK and M. MANSMANN, US Pat. 3892583 (July 1975).
10. R. H. BANEY and J. H. GAULJR, *ibid.* 4310651 (January 1982).
11. S. D. BREWER and C. P. HABER, *J. Amer. Chem. Soc.* **70** (1948) 3888.
12. D. SEYFERTH and G. H. WISEMAN, in "Ultrastructure Processing of Ceramics, Glasses and Composites", edited by L. L. Hench and D. R. Ulrich (Wiley, New York, 1984) p. 265.
13. Y. HASEGAWA and K. OKAMURA, *J. Mater. Sci.* **18** (1983) 3633.
14. K. OKAMURA, M. SATO and Y. HASEGAWA, *J. Ceram. Soc. Jpn. Inter. Edn.* **13** (1987) 55.
15. G. T. BURNS and G. CHANDRA, *J. Amer. Ceram. Soc.* **72** (1989) 333.
16. Y. HASEGAWA, *Compos. Sci. Technol.* **37** (1990) 37.

Received 7 January 1993
and accepted 21 March 1994